Check for updates

Improving and measuring the solubility of favipiravir and montelukast in SC-CO$_2$ with ethanol projecting their nanonization

Adrián Rojas,[ab] Seyed Ali Sajadian, [ID] *[c] Carol López-de-Dicastillo,[d] Nedasadat Saadati Ardestani,[e] Gonzalo Aguila [ID] [f] and Abolghasem Jouyban[gh]

Supercritical carbon dioxide (SC-CO$_2$)-based approaches have become more popular in recent years as alternative methods for creating micro- or nanosized medicines. Particularly, high drug solubility is required in those techniques using SC-CO$_2$ as a solvent. During the most recent pandemic years, favipiravir and montelukast were two of the most often prescribed medications for the treatment of COVID-19. In this study, ethanol at 1 and 3 mol% was utilized as a cosolvent to increase the solubility of both medicines in SC-CO$_2$ by a static approach using a range of temperatures (308 to 338 K) and pressure (12 to 30 MPa) values. The experimentally determined solubilities of favipiravir and montelukast in SC-CO$_2$ + 3 mol% ethanol showed solubility values up to 33.3 and 24.5 times higher than that obtained for these drugs with only SC-CO$_2$. The highest values were achieved in the pressure of 12 MPa and temperature of 338 K. Last but not least, six density-based semi-empirical models with various adjustable parameters were used to perform the modeling of the solubility of favipiravir and montelukast.

1. Introduction

Favipiravir and montelukast are two drugs whose interest has increased principally during last years because of the fact that they can be used as potential adjuvant treatments for coronavirus (COVID-19). COVID-19 is a SARS-CoV-2 virus infection, and some infected patients can become seriously ill and require medical attention. In this way, it is essential to continue looking for alternative treatments and drugs for combating this infection. Favipiravir was one of the oral drugs approved for re-emerging pandemic influenza in Japan in 2014, and recently it has demonstrated strong *in vitro* antiviral efficacy against the coronavirus that causes severe acute respiratory syndrome.[1]

aPackaging Innovation Center (LABEN), Department of Science and Food Technology, Faculty of Technology, University of Santiago of Chile (USACH), Obispo Umaña 050, Santiago 9170201, Chile

bCenter for the Development of Nanoscience and Nanotechnology (CEDENNA), Santiago 9170124, Chile

cDepartment of Chemical Engineering, Faculty of Engineering, University of Kashan, 87317-53153, Kashan, Iran. E-mail: seyedali.sajadian@gmail.com

dPackaging Laboratory, Institute of Agrochemistry and Food Technology IATA-CSIC, Av. Agustín Escardino 7, 46980 Paterna, Spain

eNanotechnology Research Center, Research Institute of Petroleum Industry (RIPI), P.O. Box: 14857-336, Tehran, Iran

fDepartamento de Ciencias de la Ingeniería, Facultad de Ingeniería, Universidad Andres Bello, Antonio Varas 880, Santiago, Chile

gPharmaceutical Analysis Research Center and Faculty of Pharmacy, Tabriz University of Medical Sciences, Tabriz, Iran

hPharmaceutical Sciences Research Center, Shahid Beheshti University of Medical Sciences, Tehran, Iran

Favipiravir (prodrug) is a selective and potent inhibitor of viral RNA-dependent RNA polymerase.[2] On the other hand, montelukast, an oral selective leukotriene receptor antagonist, is very successful in treating chronic asthma and some COVID-19 symptoms because it inhibits cysteinyl leukotriene.[3]

A drug's bioavailability, which is closely related to its solubility, determines how effectively it treats a patient. Therefore, a drug's solubility and rate of dissolution are crucial factors in determining how effective it is the drug treatment. One of the most crucial factors in achieving the correct drug concentration in the systemic circulation for the pharmacological response is solubility. Nevertheless, most drugs present poor solubility, and it is recognized that in the pharmaceutical industry more than 40% of newly discovered drugs show the same handicap.[4] Several approaches are employed to improve their bioavailability, and solubility studies and prediction tools have become a valuable information to optimize their reformulation processes. In this context, solutions taking into account the encapsulation and micronization of particles and drug delivery systems are being offered by the supercritical fluids technology.[5–7] Specifically, SC-CO$_2$ is considered a sustainable solvent as it has moderate critical parameters, is cheap, harmless, incombustible and can be recycled. Furthermore, carbon dioxide (CO$_2$) is a gas under atmospheric conditions that is easily removed from the material by simple depressurization and leaves no residue. Several life cycle assessment studies have shown the use of supercritical water and CO$_2$-based methods as sustainable processes to produce materials.[8,9] Comparing to conventional processes, the use of SC-CO$_2$ can entail da positive

Table 1 Solubility of solutes in ternary systems (SC-CO$_2$ + cosolvent + solute)

Compound	Cosolvent	Pressure range (MPa)	Temperature range (K)	Range of solubility ($\times 10^5$)	References
Capecitabine	Methanol 6 mol% Ethanol 6 mol% Dimethyl sulfoxide 6 mol%	10–35	308–348	3.18–120.29 0.64–71.9 0.85–94.8	15
Anthraquinone Violet 3RN	Methanol 6 mol%	10–34	308–338	0.44–5.77	16
Ammonium benzoate	Ethanol 2% molar Acetone 2 mol% Ethylene glycol 2 mol%	11–21	318	2.33–10.63 2.15–8.85 4.27–6.92	17
Cinnamic acid	Ethanol 2 and 4 mol%	10–40	313	23–81	18
Disperse yellow 119 Disperse red 82	Ethanol 0–5 mol%	15–30	353 and 393	0.010–3.23 0.064–110	19
Benzamide	Ethanol 3.5 mol% Acetone 3.5 mol% Ethylene glycol 3.5 mol%	11–21	318	5.79–74.83 4.93–33.99 5.07–24.03	20
Ketoconazole	Menthol (mass ratio 5 : 2 to ketoconazole)	12–30	308–338	2.7–1.96	21
Phenylphosphinic acid	Methanol 1 and 4 mol%	10–20	313 and 323	2.8–292	22
Trioctylmethylammonium chloride	n-hexane 1.05–4.20 mol%	10–30	313 and 323	1.8–15.3	23
Aspirin	Stearic acid (mass ratio 10 : 1 to aspirin)	10–20	308–328	50.5–443.9	24
Silymarin	Ethanol 2 mol% Acetone 2 mol% Dichloromethane 2 mol%	8–22	308–338	3.89–60.12 5.17–101.37 2.99–40.33	25
Nitrenpidine	Ethanol 1–7 mol%	10–20	308–318	0.18–12.55	26
Ferulic acid	Ethanol 5.37–10.92 mol%	20–40	313–333	18.9–165	27
Curcumin	Ethanol 1–5 mol%	8–16	318	0.048–0.197	28
Glycyrrhizin	Ethanol 2 and 4 mol%	9–21	308–328	0.261–5.430	29
Dexamethasone	Ethanol 3 mol%	10–25	313–323	0.197–0.298	30
Lutein	Ethanol 0.0211 mol mol^{-1}	18.70–33.55	313–333	0.402	31
Vitamin E acetate	Ethanol 0.5–2 mol%	10.99–11.13	318	38.4–69.0	32
Caffeic acid	Ethanol 2.2–10.2 mol%	20–40	313–333	5.8–9.1	33
3-Aminobenzoic acid	Ethanol 2–4 mol%	10–21	308–328	Enhancement between 1.02–2.55 times	34
o-Nitrobenzoic acid	Ethanol 3.5 mol% Ethyl acetate 3.5 mol%	10–21	308–328	0.374–3.561 0.220–1.842	35
Capsanthin	Triolein 0.16 and 0.41 mmol mol^{-1}	19–34	313–333	0.65–1.97	36
o-tolidine	Ethanol 0.01–0.04 mol% Ethylene glycol 0.01–0.04 mol%	11–21	308–328	1.01–5.99 1.11–4.25	37
Benzene sulfonamide	Ethanol 3.5 mol% Ethylene glycol 3.5 mol% Ethyl acetate 3.5 mol%	11–21	308–328	14.9–21.3 25.1–42.4 18.9–35.3	38
Acetaminophen	Menthol	10–25	313–343	1.44–24.91	39
Rhodamine B	Methanol 5 mol%	8–24	308–318	0.003372–0.076674	40
Clozapine	Menthol 8.8 mol%	12.3–33.7	313–323	18.8–44.8	41
Lamotrigine			313–323	0.9–3.6	

impact on environmental preservation, but also on economic gains, thanks to the reduction of processes time and energy expenditure, the water-free and effluent-free processes and the reduction of CO$_2$ emission and auxiliary chemicals.[10]

Specifically in the use of this technology in the development of drug delivery systems, a crucial factor in the creation of micro/nano-sized drug particles in the pharmaceutical sector is the solubility of medicinal compounds in SC-CO$_2$. Recently, data about the solubility of many pharmaceuticals in SC-CO$_2$ have been measured experimentally and published in the literature.[11,12] At pressures between 12 and 30 MPa and temperatures between 308 and 338 K, the mole fraction solubilities of favipiravir and montelukast have resulted in a range

of 3.0 × 10^{-6} to 9.05 × 10^{-4} (ref. 13) and 0.4 × 10^{-6} to 6.12 × 10^{-5},[14] respectively. Several studies have demonstrated that a strategy for improving these values is by incorporating a polar or non-polar cosolvent that can increase the solvating potential of SC-CO$_2$ perhaps lowering the operating pressure.[15–41] A selection of some relevant studies on improving the solubility of solutes in ternary systems (SC-CO$_2$ + cosolvent + solute) are included in Table 1. In a recent study, Sodeifian et al. found that employing menthol as a cosolvent increased the solubility of ketoconazole in SC-CO$_2$ at 308–338 K and 12–30 MPa from a range value between 2.00 × 10^{-7} and 8.02 × 10^{-5} to the drug solubility values of 1.20 × 10^{-5} to 1.96 × 10^{-4}.[42] Huang et al. have also improved the aspirin solubility in SC-CO$_2$ by five times

by incorporating acetone as a cosolvent.[43] Particularly, ethanol has been one of the most commonly used polar cosolvents for the solute processing (drugs and nutraceuticals)[44–46] and for the extraction of bioactive substances from plant materials[47–49] due to its high solubility in SC-CO$_2$ at moderate pressure and temperatures, low toxicity and capacity to interact with polar solutes by hydrogen bonding.

In the current work, ethanol was used for the first time as a cosolvent approved for pharmaceutical applications with the aim of improving the solubility of favipiravir and montelukast in SC-CO$_2$ and promoting further research dealing with their nanonization through techniques using SC-CO$_2$ as a solvent, such as rapid expansion of supercritical fluid solutions (RESS). In this study ethanol was used at concentrations of 1 and 3 mol% when measuring the solubilities of favipiravir and montelukast in SC-CO$_2$ at various pressures and temperatures (308–338 K) (12–30 MPa). Additionally, six density-based semi-empirical models, namely; MST,[50] Sodeifian–Sajadian,[51] González et al.,[52] Soltani–Mazloumi,[53] Garlapati–Madras,[54] and Jouyban et al.,[55] with four to seven adjustable parameters were used to correlate the solubilities of favipiravir and montelukast in both studied ternary systems. The results obtaining by modeling the solubility of these drugs in SC-CO$_2$ is orientated to facilitate the development of nanodrugs formulation processes, with the consequent saving of time and resources.

2. Experimental

2.1. Materials

Montelukast (CAS No. 158966-92-8) and favipiravir (CAS No. 259793-96-9) were bought from Arasto Pharmaceutical Chemicals Co. (Tehran, Iran). Aboughadareh Co. supplied carbon dioxide (CO$_2$) with a purity of 99.99% (CAS Number 124-38-9). (Tehran, Iran). Merck provided the methanol with a minimum purity (GC) of 99.9% and the ethanol (99.0% purity) with the CAS number 67-56-1 (Germany). The main properties of the chemicals employed in this study, which were all used without further purification, are listed in Table 2.

2.2. System for solubility determination

For the experiments carried out in this work, laboratory setup composed of different parts and equipment was used. This equipment is shown in Fig. 1 and includes a table describing its main components. The equilibrium cell, piping, and valves are constructed from 316 stainless steel and intended to operate under high pressure (40 MPa). At the beginning of the process, CO$_2$ enters the refrigeration stage to liquefy the CO$_2$ (258.15 K) and later goes through filtering (1 μm). The liquid CO$_2$ at 6 MPa is transferred using a high-pressure pump (air-driven liquid pump, type M64, Shineeast business). A pressure transmitter and a pressure gauge are used to measure the pressure with a 0.1 MPa accuracy (WIKA, Germany). To maintain a consistent operating temperature (0.1 K), the equilibrium cell was placed within a high-precision furnace (Memmert GmbH, Germany). In the equilibrium cell, 3000 mg of the drug and a specific amount of ethanol (1 or 3 mol%) are introduced as a cosolvent and mixed through a magnetic stirrer (100 rpm). At the ends of the equilibrium cell, sintered stainless steel filters were positioned to prevent the physical transfer of undissolved drug powder. More details of this laboratory equipment for experiments can be found in previous works.[56,57] Subsequently, the liquid CO$_2$ is introduced into the equilibrium cell until operating pressure is reached, and 90 min is considered for the system to reach equilibrium. After that, a 3-valve allows SC-CO$_2$ to be pumped from the equilibrium cell into a 300 μL sample loop. The sampling loop is depressurized into liquid ethanol using a micrometer valve that prevents ethanol from spraying out of the vessel. A syringe is used to introduce methanol into the sampling loop at the conclusion of the procedure. The volume of the final solution obtained in the collection vial corresponds to 5 mL. For each data point, this process is repeated three times.

The solubility of the drugs, obtained under different operating conditions of the previous process, is measured with a spectrophotometer (PerkinElmer), with quartz cells and a 3 cm path length. The amount of drug contained in the final solution, disposed in the collection vial, is measured using calibration curves. The concentration of drugs is analyzed with UV absorption analysis at maximum lambda.

The following equations were used to calculate the equilibrium solubility of the drugs in SC-CO$_2$ at all pressure and temperature ranges, including equilibrium molar fraction (y_2) and equilibrium solubility S (g L^{-1}):

$$y_2 = \frac{n_{\text{solute}}}{n_{\text{solute}} + n_{\text{CO}_2}} \tag{1}$$

where:

$$n_{\text{solute}} = \frac{C_s\left(\frac{g}{L}\right) \times V_s\,(\text{L})}{M_s\left(\frac{g}{\text{mol}}\right)} \tag{2}$$

Table 2 The sources and mass fraction purity of the materials used in present work

Material	Source	Initial mass fraction purity	Purification method	Final mass fraction purity	Analysis method
Favipiravir	Arasto pharmaceutical Co.	0.99	None	0.99	HPLC
Montelukast	Arasto pharmaceutical Co.	0.99	None	0.99	HPLC
Ethanol	Merck Co.	0.99	None	0.99	GC[a]
Methanol	Merck Co.	0.999	None	0.999	GC
CO$_2$	Aboughadareh Co.	0.9999	None	0.9999	GC

[a] Gas chromatography.
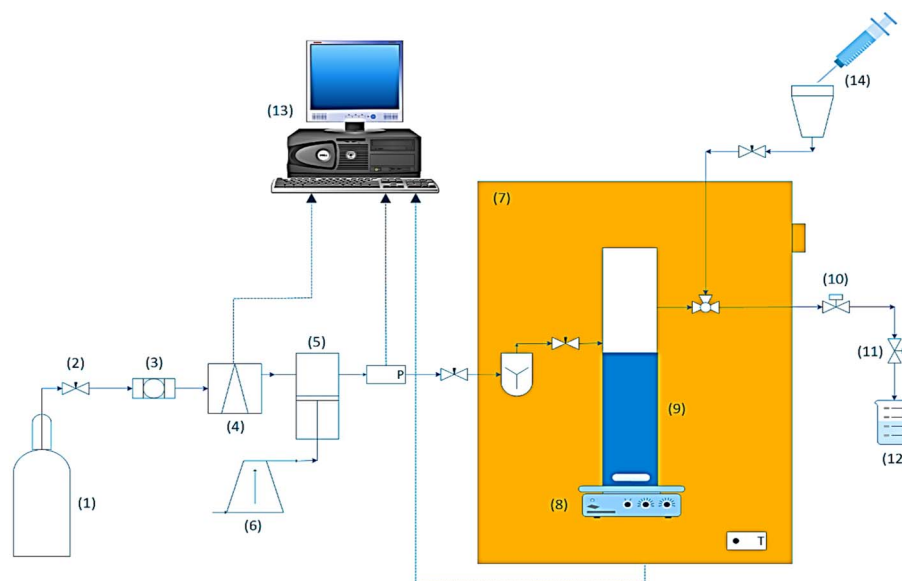
Number	Description	Material
1	Cylinder	CO_2
2	Needle valve	
3	Filter	CO_2
4	Refrigerator unit	CO_2
5	High pressure pump	CO_2
6	Compressor	air
7	Oven	
8	Magnetic stirrer	
9	Equilibrium cell	CO_2-drug
10	Back pressure	
11	Micrometer valve	
12	Collection vial	Drug
13	Control panel	
14	Syringe	Solvent

Fig. 1 Schematic diagram of experimental apparatus for measuring favipiravir and montelukast solubility.

$$n_{CO_2} = \frac{V_1(\text{L}) \times \rho\left(\frac{\text{g}}{\text{L}}\right)}{M_{CO_2}\left(\frac{\text{g}}{\text{mol}}\right)} \tag{3}$$

n_{solute} and n_{CO_2} depict the solute and CO_2 moles in the sample loop, $C_s\left(\frac{\text{g}}{\text{L}}\right)$ indicates the solute concentration in the collection vial as calculated by the calibration curve, V_s (L) and V_1 (L) show the collection vial and sample loop volumes, and $M_s\left(\frac{\text{g}}{\text{mol}}\right)$ and $M_{CO_2}\left(\frac{\text{g}}{\text{mol}}\right)$ reflect the solute's and CO_2's molecular weights, respectively. Eqn (4) is produced by adding eqn. (2) and (3) to eqn (1):

$$y_2 = \frac{C_s\left(\frac{\text{g}}{\text{L}}\right) \times V_s\,(\text{L}) \times M_{CO_2}\left(\frac{\text{g}}{\text{mol}}\right)}{C_s\left(\frac{\text{g}}{\text{L}}\right) \times V_s(\text{L}) \times M_{CO_2}\left(\frac{\text{g}}{\text{mol}}\right) + V_1(\text{L}) \times \rho\left(\frac{\text{g}}{\text{L}}\right) \times M_s\left(\frac{\text{g}}{\text{mol}}\right)} \tag{4}$$

Eqn (5) also yielded the equilibrium solubility, S (g L^{-1}), of the solute in SC-CO_2.

$$S\left(\frac{\text{g}}{\text{L}}\right) = \frac{C_s\left(\frac{\text{g}}{\text{L}}\right) \times V_s(\text{L})}{V_1(\text{L})} \tag{5}$$
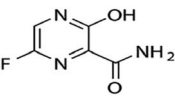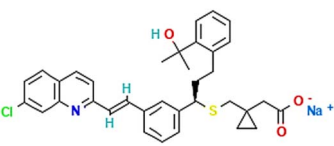
Information on API's physical characteristics can be found in Table 3. The National Institute of Standards and Technology (NIST) database was used to determine the density (ρ) for SC-CO_2 at various temperatures and pressures.

3. Theoretical background

According to Mendez-Santiago–Teja (MST),[50] Sodeifian–Sajadian,[51] González et al.,[52] Soltani–Mazloumi,[53] Garlapati and Madras,[54] and, Jouyban et al.,[55] empirical models based on density were utilized in this study. These empirical models allowed to correlate the experimentally obtained solubility data.

Table 3 The utilized solute structure and the respective physical-chemical features (M_w: molecular weight, T_m: melting point, λ_{max}: λ with maximum absorbance)

Compound	Formula	Structure	M_W (g mol^{-1})	CAS number	T_m (K)	λ_{max} (nm)
Favipiravir	$C_5H_4FN_3O_2$		157.1	259793-96-9	465.9	323
Montelukast sodium	$C_{35}H_{35}ClNO_3S\ Na$		608.20	151767-02-1	419.20	281

In addition, the constants of these empirical models were obtained through a regression of the experimental data. Finally, using simulated annealing (MATLAB®), it was possible to obtain the adjustable parameters.

Since correlations based on density can be used to explain the solubility of solids in supercritical fluids (SCF), empirical models based on density were used. Since these empirical models depend on the pressure, temperature, and SCF density, which correspond to independent variables, in addition to constants and adjustable parameters, they have the advantage of not requiring estimation of the physicochemical features of the solid.

Table 4 The experimental data of favipiravir solubility in SC-CO$_2$ (binary system) and SC-CO$_2$ with 1 mol% of ethanol (ternary system) at different conditions of temperature and pressure[a]

Temperature[b] (K)	Pressure[b] (MPa)	Binary $y_2 \times 10^4$ (mole fraction)[c]	Ternary $y'_2 \times 10^3$ (mole fraction)	Experimental standard deviation, $S\ (\bar{y}') \times 10^4$	e (cosolvent effect)
308	12	0.53	0.50	0.10	9.43
	15	0.87	0.70	0.17	8.05
	18	1.44	1.00	0.30	7.14
	21	2.31	1.40	0.43	6.06
	24	3.42	1.60	0.77	4.68
	27	4.09	1.80	0.93	4.40
	30	5.13	2.00	1.23	3.90
318	12	0.37	0.30	0.08	8.11
	15	0.80	0.60	0.22	7.50
	18	1.30	0.70	0.41	5.38
	21	2.72	1.30	0.78	4.78
	24	4.29	2.00	1.30	4.66
	27	5.41	2.40	1.34	4.44
	30	6.48	2.80	1.50	4.32
328	12	0.08	0.09	0.01	11.25
	15	0.60	0.50	0.10	8.33
	18	1.39	1.00	0.33	7.19
	21	3.21	1.80	0.88	5.61
	24	4.75	2.50	1.39	5.26
	27	6.58	3.00	1.18	4.56
	30	7.65	3.40	1.49	4.44
338	12	0.03	0.06	0.03	20.00
	15	0.37	0.50	0.20	13.51
	18	1.32	1.10	0.78	8.33
	21	3.92	2.30	1.05	5.87
	24	5.6	3.00	1.59	5.36
	27	7.57	3.90	2.05	5.15
	30	9.05	4.40	2.40	4.86

[a] y_2, y'_2 and e are molar fraction of favipiravir in SC-CO$_2$ (binary system), in SC-CO$_2$ with 1% of ethanol, and the cosolvent effect, respectively. [b] For each experimental run cosolvent effect was calculated as $y_2/$, y'_2. Standard uncertainty u are $u(T) = 0.1$ K; $u(p) = 1$ bar. Also, the relative standard deviations are obtained below 0.05 for mole fractions and solubilities. [c] Data taken from a previous work.[13]

Through the establishment of two trustworthy statistical criteria, Average Absolute Relative Deviation (AARD%) and correlation coefficient (R_{adj}), were used to evaluate the performance of the thermodynamics models employed in this investigation to correlate the solubility of both medicines in SC-CO$_2$ with ethanol at 1 and 3 mol% was assessed:[58]

$$AARD\% = \frac{100}{N_t - Z} \sum_{i=1}^{N_t} \frac{|y_2^{cal} - y_2^{exp}|}{y_2^{exp}} \qquad (6)$$

The experimental value of the molar solubility of favipiravir and montelukast in SC-CO$_2$ with ethanol at 1 and 3 mol% is represented by y_{exp} in eqn (6). The theoretical solubility values determined using the suggested thermodynamics models are represented by y_{cal} in the meanwhile.

$$R_{adj} = \sqrt{|R^2 - (Q(1 - R^2)/(N - Q - 1))|} \qquad (7)$$

R_{adj} was calculated according eqn (7). In eqn (7) N is the data points number for each set, and Q correspond to the number of independent variables.

4. Results and discussion

4.1. Experimental solubility data

To validate the equipment used to determine the solubility of favipiravir and montelukast in SC-CO$_2$, in a previous work,[59] the solubility of capecitabine and naphthalene at different temperatures and pressures was determined, using the same equipment that in this study, and compared with existing data reported by Amani *et al.*,[60] Iwai *et al.*,[61] Ardestani *et al.*,[15] and Sodeifian *et al.*[62]

Our research team has previously published data on the solubility of favipiravir[13] and montelukast[14] in SC-CO$_2$ reported as molar fraction at various temperatures (308 to 338 K) and pressures (12 to 30 MPa) in the range of 0.03×10^{-4} to 9.00×10^{-4} and 0.04×10^{-5} to 6.12×10^{-5}, respectively. In the current study, ethanol was utilized as a cosolvent to increase these medicines' solubility in SC-CO$_2$. To improve the precision of the measurements, every experimental run was developed in triplicates. The experimental molar solubility values for favipiravir and montelukast in SC-CO$_2$ with 1 and 3 mol% ethanol is shown in Tables 4 and 5, and 6 and 7, respectively. From these

Table 5 The experimental data of favipiravir solubility in SC-CO$_2$ (binary system) and SC-CO$_2$ with 3 mol% of ethanol (ternary system) at different conditions of temperature and pressure[a]

Temperature[b] (K)	Pressure[b] (MPa)	Binary $y_2 \times 10^4$ (mole fraction)[c]	Ternary $y'_2 \times 10^3$ (mole fraction)	Experimental standard deviation, $S(\bar{y}') \times 10^4$	e (cosolvent effect)
308	12	0.53	0.61	0.11	11.32
	15	0.87	0.80	0.16	9.20
	18	1.44	1.21	0.29	8.57
	21	2.31	1.50	0.42	6.49
	24	3.42	2.20	0.73	6.43
	27	4.09	2.50	0.93	6.11
	30	5.13	2.91	1.20	5.65
318	12	0.37	0.42	0.10	10.81
	15	0.80	0.80	0.23	10.00
	18	1.30	1.22	0.39	9.23
	21	2.72	2.20	0.79	8.09
	24	4.29	3.10	1.32	7.23
	27	5.41	3.60	1.30	6.65
	30	6.48	3.80	1.52	5.86
328	12	0.08	0.12	0.02	12.50
	15	0.60	0.71	0.14	11.67
	18	1.39	1.50	0.36	10.79
	21	3.21	3.01	0.84	9.35
	24	4.75	3.83	1.33	8.00
	27	6.58	4.80	1.15	7.29
	30	7.65	5.13	1.48	6.67
338	12	0.03	0.10	0.03	33.33
	15	0.37	0.60	0.22	16.22
	18	1.32	1.90	0.76	14.39
	21	3.92	3.81	1.07	9.69
	24	5.6	4.90	1.57	8.75
	27	7.57	5.72	2.06	7.53
	30	9.05	6.10	2.44	6.74

[a] y_2, y'_2 and e are molar fraction of favipiravir in SC-CO$_2$ (binary system), in SC-CO$_2$ with 3% of ethanol, and the cosolvent effect, respectively [b] For each experimental run cosolvent effect was calculated as y_2/y'_2. Standard uncertainty u are $u(T) = 0.1$ K; $u(p) = 0.1$ MPa. Also, the relative standard deviations are obtained below 0.05 for mole fractions and solubilities. [c] Data taken from a previous work.[13]

results, it can be seen that the addition of ethanol at 1 and 3 mol% increased the solubility of drugs under all the pressure and temperature parameters examined because the polarity of supercritical mixture's is increased. The solubility of other compounds in SC-CO$_2$ has been reported to be affected by the addition of ethanol in the same way. Li *et al.* reported a 6.87-fold increase in benzamide solubility in SC-CO$_2$ using ethanol at 3.5 mol% at 318 K and 18 MPa.[20] Lee *et al.* reported 5.77 and 15.74-fold increase in the solubility of modified disperse yellow 119 and red 82 in SC-CO$_2$ at 353.2 K, 30 MPa and using ethanol 3 mol% as cosolvent, respectively.[19] Meanwhile, Ota *et al.* reported a 5.16-fold increase in the solubility of anthracene in SC-CO$_2$ at 333 K, 22 MPa and using ethanol 3 mol% as a cosolvent.[63] Li *et al.* reported a 2.96-fold increase in the solubility of *p*-toluenesulfonamide in SC-CO$_2$ at 328 K, 21 MPa and using ethanol 3.5% as a cosolvent.[64]

In this study, the solubility of favipiravir and montelukast in the SC-CO$_2$ was experimentally investigated at various pressures and temperatures (308 to 338 K) (12 to 30 MPa) and reported in the range of 0.1×10^{-4} to 6.1×10^{-3} and 0.1×10^{-4} to 3.59×10^{-4}, respectively for 3 mol%, which corresponded to solubility

values up to 33.3 and 24.5 times higher than the obtained for these substances using pure SC-CO$_2$ (Tables 5 and 7). Furthermore, the results in Tables 4 and 6 showed that by adding ethanol 1 mol% to SC-CO$_2$, the solubility of favipiravir and montelukast increased 20 and, 9.5 times respectively, and mole fractions of drugs were in the range of 0.60×10^{-5} to 4.40×10^{-3} and 0.38×10^{-5} to 17.05×10^{-5}.

Particularly, the improvement in the solubility of both substances can be related to the presence of hydrogen donors and acceptors moieties in their structures in which ethanol was able to interact with those molecules by hydrogen bonding.[65] The largest solubility of favipiravir and montelukast in SC-CO$_2$ with ethanol 1 and 3 mol% was obtained at the highest values of temperature (338 K) and pressure (30 MPa). At these conditions, the molar solubility of favipiravir (6.1×10^{-3}) was 17 times higher than the obtained for montelukast (3.59×10^{-4}) which agreed with the reported 15 times higher solubility of favipiravir than the reported for montelukast in SC-CO$_2$ under same pressure and temperature conditions.[13,14]

The solubility of favipiravir and montelukast in a mixture of SC-CO$_2$ and 3 mol% ethanol is depicted in Fig. 2 as a function of

Table 6 The experimental data of montelukast solubility in SC-CO$_2$ (binary system) and SC-CO$_2$ with 1 mol% of ethanol (ternary system) at different conditions of temperature and pressure[a]

| Temperature[b] (K) | Pressure[b] (MPa) | Binary | Ternary | | |
		$y_2 \times 10^5$ (molar fraction)[c]	$y'_2 \times 10^5$ (mole fraction)	Experimental standard deviation, $S(\bar{y}') \times 10^5$	e (cosolvent effect)
308	12	0.13	0.68	0.03	5.23
	15	0.24	1.03	0.04	4.29
	18	0.36	1.47	0.07	4.08
	21	0.48	1.71	0.08	3.56
	24	0.61	2.03	0.09	3.33
	27	0.74	2.26	0.14	3.05
	30	0.88	2.52	0.16	2.86
318	12	0.10	0.49	0.02	4.90
	15	0.22	1.02	0.06	4.64
	18	0.58	2.20	0.11	3.79
	21	0.89	3.25	0.19	3.65
	24	1.22	3.89	0.23	3.19
	27	1.57	4.64	0.27	2.96
	30	1.94	5.50	0.30	2.84
328	12	0.07	0.42	0.01	6.00
	15	0.20	1.00	0.03	5.00
	18	0.76	3.52	0.14	4.63
	21	1.38	5.67	0.27	4.11
	24	2.12	7.40	0.40	3.49
	27	2.94	10.02	0.41	3.41
	30	3.83	11.72	0.56	3.06
338	12	0.04	0.38	0.02	9.50
	15	0.16	0.92	0.06	5.75
	18	0.77	4.18	0.30	5.43
	21	1.81	8.09	0.32	4.47
	24	3.20	10.13	0.63	3.17
	27	4.73	14.00	1.02	2.96
	30	6.12	17.05	1.45	2.79

[a] y_2, y'_2 and e are molar fraction of montelukast in SC-CO$_2$ (binary system), in SC-CO$_2$ with 1% of ethanol, and the cosolvent effect, respectively. [b] For each experimental run cosolvent effect was calculated as y_2/y'_2. Standard uncertainty u are $u(T) = 0.1$ K; $u(p) = 0.1$ MPa. Also, the relative standard deviations are obtained below 0.05 for mole fractions. [c] Data taken from a previous work.[14]

Table 7 The experimental data of montelukast solubility in SC-CO$_2$ (binary system) and SC-CO$_2$ with 3 mol% of ethanol (ternary system) at different conditions of temperature and pressure[a]

| Temperature[b] (K) | Pressure[b] (MPa) | Binary | Ternary | | |
		$y_2 \times 10^5$ (molar fraction)[c]	$y'_2 \times 10^4$ (mole fraction)	Experimental standard deviation, $S(\bar{y}') \times 10^5$	e (cosolvent effect)
308	12	0.13	0.11	0.02	8.4
	15	0.24	0.16	0.03	6.8
	18	0.36	0.23	0.06	6.3
	21	0.48	0.26	0.08	4.8
	24	0.61	0.30	0.10	4.7
	27	0.74	0.34	0.13	4.5
	30	0.88	0.38	0.16	4.1
318	12	0.10	0.08	0.02	7.9
	15	0.22	0.16	0.05	7.4
	18	0.58	0.33	0.11	6.8
	21	0.89	0.49	0.18	6.0
	24	1.22	0.58	0.25	5.3
	27	1.57	0.69	0.25	4.9
	30	1.94	0.81	0.32	4.2
328	12	0.07	0.06	0.01	9.1
	15	0.20	0.17	0.03	8.6
	18	0.76	0.60	0.14	7.9
	21	1.38	0.94	0.27	6.8
	24	2.12	1.25	0.43	5.9
	27	2.94	1.55	0.39	5.3
	30	3.83	1.86	0.54	4.9
338	12	0.04	0.10	0.03	24.5
	15	0.16	0.19	0.07	11.8
	18	0.77	0.81	0.32	10.5
	21	1.81	1.29	0.36	7.1
	24	3.20	2.03	0.65	6.4
	27	4.73	2.80	1.01	5.7
	30	6.12	3.59	1.44	4.9

[a] y_2, y'_2 and e are molar fraction of montelukast in SC-CO$_2$ (binary system), in SC-CO$_2$ with 3% of ethanol, and the cosolvent effect, respectively. [b] For each experimental run cosolvent effect was calculated as y_2/y'_2. Standard uncertainty u are $u(T) = 0.1$ K; $u(p) = 0.1$ MPa. Also, the relative standard deviations are obtained below 0.05 for mole fractions and solubilities. [c] Data taken from a previous work.[14]

operational factors (pressure, temperature, and density). As shown by the isotherms in Fig. 2, the solubility of favipiravir (Fig. 2a) and montelukast (Fig. 2c) in the supercritical mixture increased considering all the temperatures utilized in this study with rising pressure because of the well-known improvement of the solvent power of SC-CO$_2$ as pressure rise isothermally due to the increase of density. Azim *et al.* reported the increase in the solubility of ibuprofen and ketoprofen as pressure raised from 8.5 MPa to 40 MPa at different constant temperature values.[66] Ardestani *et al.* reported the increase in chloroquine's solubility in SC-CO$_2$ as pressure raised from 12 to 40 MPa at different temperatures.[67] The crossover pressure region for favipiravir in the SC-CO$_2$ ethanol mixture was shown experimentally in Fig. 2a to be between 15 and 18 MPa, which was lower than the crossover region previously reported for favipiravir in pure SC-CO$_2$.[13] This crossover reduction by using a cosolvent has been reported for several drugs.[51,68] This meant that the solubility of favipiravir increased as the temperature increased isobarically in both SC-CO$_2$ and mixtures of 3 mol% ethanol and pure SC-CO$_2$ using pressure values over the crossover region because the increase in favipiravir's vapor pressure was dominant over the

adverse effect of decreasing CO$_2$ density on solubility. The solubility of favipiravir, on the other hand, dropped when the temperature increased isobarically below the crossover zone since the negative influence of decreasing density over solubility was dominating. A similar crossover pressure region has been reported for haloperidol[69] and ketoprofen.[70] For montelukast, a little reduction in its crossover pressure from 15–16 MPa (binary system) to 15 MPa (ternary system) was obtained due to the use of ethanol 3 mol%.

4.2. Correlation of the solubility data with semi-empirical models

The solubility of favipiravir and montelukast in the two examined ternary systems (favipiravir-SC-CO$_2$-ethanol and montelukast-SC-CO$_2$-ethanol) was correlated in this investigation using six empirical density-based models with four to seven adjustable parameters (MST, Sodeifian–Sajadian, González *et al.*, Soltani–Mazloumi, Garlapati–Madras, and Jouyban *et al.*). Table 8 shows the equations associated to each density-based model used in the present research. The average absolute relative deviation (AARD%), correlation coefficient (R_{adj}) and the
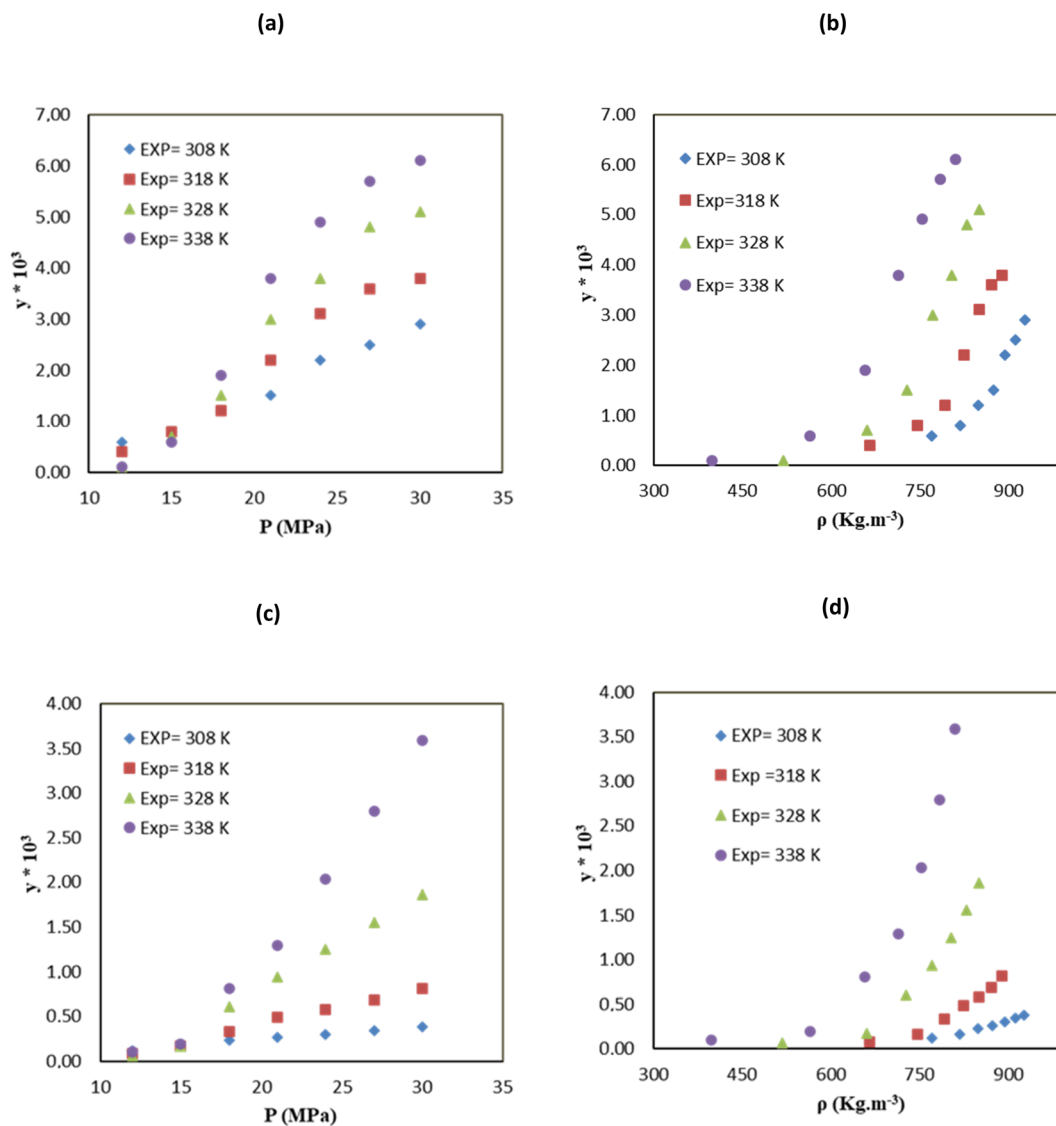
(a)

(b)

(c)

(d)

Fig. 2 The influence of pressure and density of the SC-CO$_2$ + 3 mol% ethanol mixture on favipiravir (a and b) and montelukast (c and d) solubility at different temperatures.

Table 8 A brief statement of the density-based models utilized in the present research (ρ_1, T, P, P_{ref}, y'_2, y_3 and a_0–a_6 are density of SC-CO$_2$, temperature, pressure, reference pressure, mole fraction in ternary system, mole fraction of cosolvent and adjustable parameters, respectively)

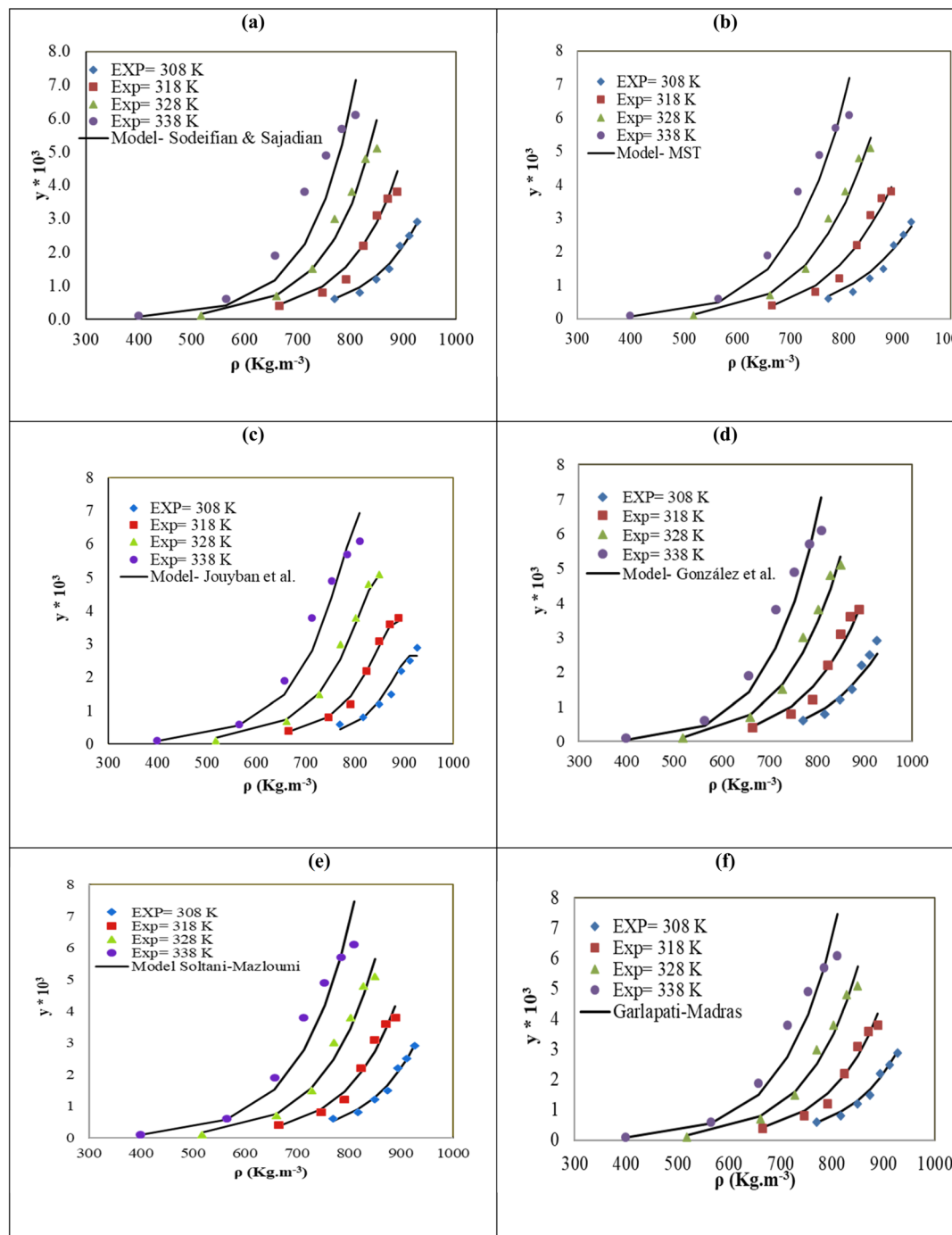| Model	Formula
MST[50]	$T\ln\left(\dfrac{y'_2 P}{P_{ref}}\right) = a_0 + a_1\rho_1 + a_2 T + a_3 y_3$
Sodeifian–Sajadian[51]	$\ln(y'_2) = \left(a_0 + \dfrac{a_1\rho_1}{T}\right)\ln(\rho_1) + a_2\rho_1 + a_3\ln(y_3 P)$
González et al.[52]	$\ln(y'_2) = a_0\ln(\rho_1) + a_1\ln(y_3) + \dfrac{a_2}{T} + a_3$
Soltani–Mazloumi[53]	$\ln(y'_2) = a_0 + \dfrac{a_1}{T} + \dfrac{a_2}{T}\rho_1 - a_3\ln(P) + a_4\ln(y_3\rho_1 T)$
Garlapati–Madras[54]	$\ln(y'_2) = a_0 + a_1\ln(\rho_1) + a_2\rho_1 + \dfrac{a_3}{T} + a_4\ln(T) + a_5\ln(y_3) + a_6\ln(y_3\rho_1 T)$
Jouyban et al.[55]	$\ln(y'_2) = a_0 + a_1 y_3 + a_2\rho_1 + a_3 P^2 + a_4 PT + a_5\dfrac{T}{P} + a_6\ln(\rho_1)$

Fig. 3 Experimental (points) and calculated (line) solubility values of favipiravir in SC-CO$_2$ + 3 mol% ethanol mixture at different temperatures using (a) Sodeifian & Sajadian, (b) the dilute solution-based MST model, (c) Soltani–Mazloumi, (d) González et al., (e) Jouyban et al., (f) Garlapati–Madras.

adjustable parameters obtained for each model through their correlation with the experimental solubility data of favipiravir and montelukast in SC-CO$_2$ with ethanol 1 and 3 mol% are shown in Tables 9 and 10 respectively. Additionally, Fig. 3a–f and Fig. 4a–f, respectively, depict the experimental (points) and computed data (line) of the solubility of favipiravir and montelukast in SC-CO$_2$ based on empirical models at various pressures and temperatures and 3 mol% cosolvent.

The correlation of the solubility of favipiravir in the ternary systems using various models yielded correlation coefficient (R_{adj}) and AARD% higher than 0.9691, and lower than 15.91%, respectively, demonstrating that each model taken into consideration in this study has adequate accuracy to represent the solubility of favipiravir in SC-CO$_2$ with 1 and 3 mol% of ethanol. The MST model performed the best to correlate the solubility of favipiravir, according the results shown in Table 9,
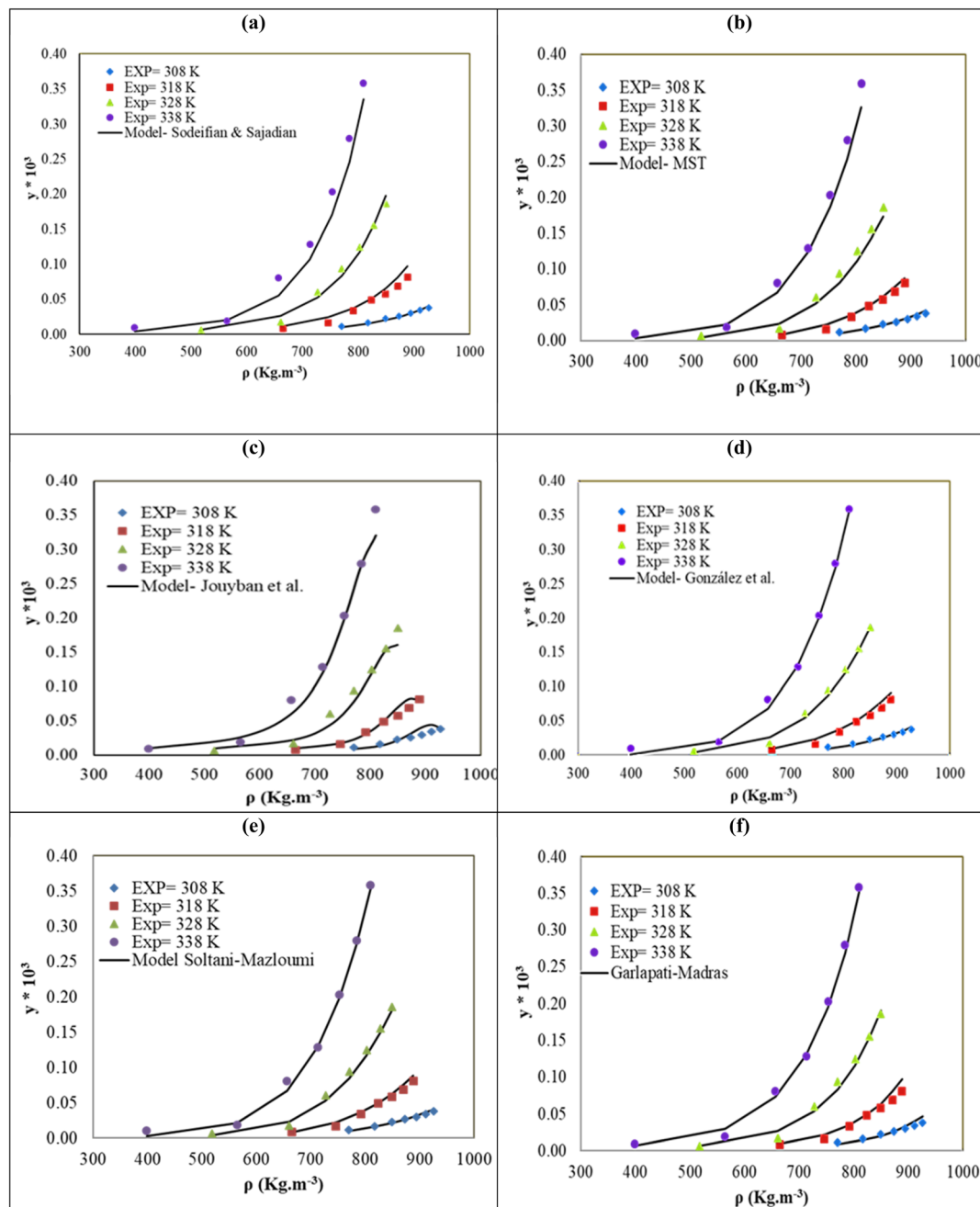
Fig. 4 Experimental (points) and calculated (line) solubility values of montelukast in SC-CO_2 + 3 mol% ethanol mixture at different temperatures using (a) Sodeifian–Sajadian, (b) the dilute solution -based MST model, (c) Jouyban *et al.*, (d) González *et al.*, (e) Soltani–Mazloumi, (f) Garlapati–Madras.

in the ternary system due to presented a lower AARD% than the values obtained for the other semi-empirical models with the same number of adjustable parameters (González *et al.* and Sodeifian–Sajadian) and even to those obtained using the models with a higher number of adjustable parameters (Garlapati–Madras and Jouyban *et al.*). The more accuracy of the MST model has been previously reported for the correlation of the solubility of different solutes in SC-CO_2. Esfandiari & Sajadian showed that the MST had a good degree of accuracy for simulating the solubility of glibenclamide in SC-CO_2 at temperatures and pressures between 12 and 30 MPa and

between 308 and 338 K, respectively.[59] In order to correlate the solubility of paracetamol in SC-CO_2 at pressure and temperature values ranging from 9.5 to 26.5 MPa and 311 to 358 K, respectively, Bagheri *et al.* found that the MST model was the most effective.[71] The same predicting capacity of the MST model was reported by Zabihi *et al.* to estimate salsalate solubility in SC-CO_2.[72]

The reported R_{adj} and AARD% values, on the other hand, resulted from the correlation of montelukast solubility in the ternary system using several semi-empirical density models, were in the range of 0.9691–0.9894, and 11.77–15.91%

Table 9 The correlation results of the favipiravir-SC-CO$_2$- ethanol system provided by the semi empirical models (AARD, R_{adj} and a_0-a_6 are average absolute relative deviation, adjusted correlation coefficient and adjustable parameters, respectively)

Model	a_0	a_1	a_2	a_3	a_4	a_5	a_6	AARD%	R_{adj}
MST	−13098.6	4.45	28.37	−5404	—	—	—	11.77	0.9894
González et al.	7.30	0.298	−7068.52	−31.91	—	—	—	14.92	0.9763
Sodeifian–Sajadian	−2.82	−1.167	0.0404	0.339	—	—	—	15.19	0.9691
Soltani–Mazloumi	−15.91	−1048.61	3.337	0.118	0.348	—	—	11.83	0.9886
Garlapati–Madras	−52.0	−3.68	0.008	4676.79	3.53	−4.39	4.73	12.86	0.9849
Jouyban et al.	−46.128	19.14	−0.0041	−0.0069	0.00131	0.037	5.451	12.49	0.9862

Table 10 The correlation results of the montelukast-SC-CO$_2$- ethanol system provided by the semi empirical models (AARD, R_{adj} and a_0-a_6 are average absolute relative deviation, adjusted correlation coefficient and adjustable parameters, respectively)

Model	a_0	a_1	a_2	a_3	a_4	a_5	a_6	AARD%	R_{adj}
MST	−16990	4.45	36.61	−7281.9				14.76	0.9921
González et al.	7.59	0.44	−11179.5	−24.31				15.37	0.9913
Sodeifian–Sajadian	−3.53	−1.7924	0.0549	0.474	—	—	—	16.27	0.9892
Soltani–Mazloumi	−33.82	−17794.1	4.71	1.27	0.43			14.65	0.9918
Garlapati–Madras	−41.63	−3.10	0.0121	−7961.1	15.01	−4.71	0.031	15.95	0.9901
Jouyban et al.	−27.88	29.19	0.0033	−0.0133	0.0025	0.199	0.031	17.11	0.9854

respectively. This result showed that various semi-empirical models correctly predicted montelukast's solubility in SC-CO$_2$ with 1 and 3 mol% of ethanol at pressures and temperatures ranging from 12 to 30 MPa and 308 to 338 K, respectively. According to the results presented in Table 10, in this case the MST model also presented a better performance than the obtained using the semi-empirical models with more adjustable parameters to estimate montelukast's solubility in the ternary system due to presented the lowest AARD% value.

5. Conclusions

In this study, the increase in solubility of favipiravir and montelukast in SC-CO$_2$ using ethanol 3 mol% as cosolvent was determined for the first time by spectrophotometric assays following a static method. The use of ethanol as a cosolvent increased the solubility of favipiravir and montelukast for all the studied conditions of pressure and temperature due to the increase of the polarity of the supercritical mixture. The highest solubility of favipiravir and montelukast in the ternary system (3 mol% ethanol) at different temperature (308 to 338 K) and pressure values (12 to 30 MPa) were in the range of 0.1×10^{-4} to 6.1×10^{-3} and 0.1×10^{-4} to 3.59×10^{-4}, respectively, which correspond to solubility values up to 33.33 and 24.5 times higher than the obtained for these substances using pure SC-CO$_2$. The solubility of both drugs increased with increasing pressure for all the temperatures used in this study due to the well-known improvement of the solvent power of SC-CO$_2$ as pressure rise isothermally due to the increase of density. The highest solubility of favipiravir and montelukast in the ternary systems were obtained at the highest values of temperature (338 K) and pressure (30 MPa) and 3 mol% of ethanol as cosolvent. The experimental solubility of favipiravir and montelukast was correlated with six density-based semi-empirical models with different adjustable parameters (González et al., Mendez-Santiago–Teja, Garlapati, and Madras, Sodeifian–Sajadian, Soltani–Mazloum and Jouyban et al.). The MST model presented the best performance to correlate the solubility of favipiravir (AARD%: 11.77% and R_{adj}: 0.9894) and montelukast (AARD%: 14.65% and R_{adj}: 0.9918) in the ternary systems.

The solubility data obtained in this study aims to support the future development of nano formulations of favipiravir and montelukast with improved solubility, bioavailability and consequently pharmacological activity by the selection of an adequate nanonization method based in supercritical carbon dioxide.

Conflicts of interest

There are no conflict to declare.

Acknowledgements

References

1 S. Joshi, J. Parkar, A. Ansari, A. Vora, D. Talwar, M. Tiwaskar, S. Patil and H. Barkate, *Int. J. Infect. Dis.*, 2021, **102**, 501–508.

2 T. Baranovich, S.-S. Wong, J. Armstrong, H. Marjuki, R. J. Webby, R. G. Webster and E. A. Govorkova, *J. Virol.*, 2013, **87**, 3741–3751.

3 J. Barré, J. M. Sabatier and C. Annweiler, *Front. Pharmacol*, 2020, **11**, 1344.

4 Introduction to Biopharmaceutics and Pharmacokinetics | Applied Biopharmaceutics & Pharmacokinetics, 7e|AccessPharmacy|McGraw Hill Medical, **https://accesspharmacy.mhmedical.com/content.aspx?sectionid=100668900&bookid=1592**, accessed 4 December 2022.

5 R. K. Kankala, P. Y. Xu, B. Q. Chen, S. Bin Wang and A. Z. Chen, *Adv. Drug Delivery Rev.*, 2021, **176**, 113846.

6 E. Velásquez, C. Patiño Vidal, A. Rojas, A. Guarda, M. J. Galotto and C. López de Dicastillo, *Compr. Rev. Food Sci. Food Saf.*, 2021, **20**, 3388–3403.

7 A. Rojas, A. Torres, M. J. Galotto, A. Guarda and R. Julio, *Crit. Rev. Food Sci. Nutr.*, 2020, **60**, 1290–1301.

8 S. Yu, X. Dong, P. Zhao, Z. Luo, Z. Sun, X. Yang, Q. Li, L. Wang, Y. Zhang and H. Zhou, *Nat. Commun.*, 2022, **13**, 3616.

9 S. Yu, P. Zhao, X. Yang, Q. Li, Y. Zhang and H. Zhou, *Fuel*, 2022, **326**, 124997.

10 C. R. S. de Oliveira, P. V. de Oliveira, L. Pellenz, C. R. L. de Aguiar and A. H. da S. Júnior, *J. Environ. Sci.*, 2023, DOI: **10.1016/J.JES.2023.06.007**.

11 S. A. Sajadian, H. Peyrovedin, K. Zomorodian and M. Khorram, *J. Supercrit. Fluids*, 2023, **194**, 105858.

12 G. Sodeifian, F. Razmimanesh and S. A. Sajadian, *J. Supercrit. Fluids*, 2019, **146**, 89–99.

13 S. A. Sajadian, N. S. Ardestani, N. Esfandiari, M. Askarizadeh and A. Jouyban, *J. Supercrit. Fluids*, 2022, **183**, 105539.

14 S. A. Sajadian, N. S. Ardestani and A. Jouyban, *J. Mol. Liq.*, 2022, **349**, 118219.

15 N. S. Ardestani, N. Y. Majd and M. Amani, *J. Chem. Eng. Data*, 2020, **65**, 4762–4779.

16 N. Saadati Ardestani, M. Amani and L. Moharrery, *Chem. Eng. Res. Des.*, 2020, **159**, 529–542.

17 B. Li, K. Liu, J. Zhu, Y. Wang, H. Meng and J. Jin, *J. Chem. Eng. Data*, 2022, **67**, 689–694.

18 A. Cháfer, T. Fornari, R. P. Stateva and A. Berna, *J. Chem. Eng. Data*, 2009, **54**, 2263–2268.

19 M. J. Lee, C. C. Ho, H. M. Lin, P. Y. Wang and J. S. Lu, *J. Supercrit. Fluids*, 2014, **95**, 258–264.

20 J. L. Li, J. S. Jin, Z. T. Zhang and Y. B. Wang, *Fluid Phase Equilib.*, 2011, **307**, 11–15.

21 G. Sodeifian, S. A. Sajadian, F. Razmimanesh and S. M. Hazaveie, *Sci. Rep.*, 2021, **11**(1), 7546, DOI: **10.1038/s41598-021-87243-6**.

22 D. John, C. P. Kancharlapalli and S. Nagarajan, *J. Chem. Eng. Data*, 2019, **64**, 5775–5784.

23 K. C. Pitchaiah, N. Lamba, N. Sivaraman and G. Madras, *J. Supercrit. Fluids*, 2018, **138**, 102–114.

24 H. Behjati Rad, J. Karimi Sabet and F. Varaminian, *Chem. Eng. Technol.*, 2019, **42**, 1259–1267.

25 G. Yang, Z. Li, Q. Shao and N. Feng, *Asian J. Pharm. Sci.*, 2017, **12**, 456–463.

26 S. Zhan, L. Cui, Q. Zhao, L. Chen, J. Wang, S. Chen and S. Ding, *J. Solution Chem.*, 2015, **44**, 1–15.

27 R. G. Bitencourt, F. A. Cabral and A. J. A. Meirelles, *J. Chem. Thermodyn.*, 2016, **103**, 285–291.

28 S. Zhan, S. Li, Q. Zhao, W. Wang and J. Wang, *J. Chem. Eng. Data*, 2017, **62**, 1257–1263.

29 J. F. Jia, F. Zabihi, Y. H. Gao and Y. P. Zhao, *J. Chem. Eng. Data*, 2015, **60**, 1744–1749.

30 C. Tang, Y. X. Guan, S. J. Yao and Z. Q. Zhu, *J. Chem. Eng. Data*, 2014, **59**, 3359–3364.

31 K. A. Araus, V. Casado, J. M. del Valle, P. S. Robert and J. C. de la Fuente, *J. Supercrit. Fluids*, 2019, **143**, 205–210.

32 J. Cheng, S. Han, J. Song, W. Wang and Z. Jiao, *J. Chem. Eng. Data*, 2018, **63**, 4248–4255.

33 R. G. Bitencourt, A. M. Palma, J. A. P. Coutinho, F. A. Cabral and A. J. A. Meirelles, *J. Supercrit. Fluids*, 2018, **138**, 238–246.

34 Y. Li, Y. Ning, J. Jin and Z. Zhang, *J. Chem. Eng. Data*, 2013, **58**, 2176–2180.

35 J. S. Jin, Z. M. Dou, H. H. Liu, H. Wu and Z. T. Zhang, *J. Chem. Eng. Data*, 2012, **57**, 2217–2220.

36 K. A. Araus, J. M. Del Valle, P. S. Robert and J. C. De La Fuente, *J. Chem. Thermodyn.*, 2012, **51**, 190–194.

37 J. S. Jin, Z. M. Dou, G. X. Su, Z. T. Zhang and H. T. Liu, *Fluid Phase Equilib.*, 2012, **315**, 9–15.

38 J. S. Jin, Y. B. Wang, Z. T. Zhang and H. T. Liu, *Thermochim. Acta*, 2012, **527**, 165–171.

39 J. Karimi Sabet, C. Ghotbi, F. Dorkoosh and A. Striolo, *Sci. Iran.*, 2012, **19**, 619–625.

40 C. Zhao, J. B. Wang, I. Tabata and T. Hori, *Adv. Mater. Res.*, 2011, **332–334**, 146–151.

41 M. H. Hosseini, N. Alizadeh and A. R. Khanchi, *J. Supercrit. Fluids*, 2010, **55**, 14–22.

42 G. Sodeifian, S. A. Sajadian, F. Razmimanesh and S. M. Hazaveie, *Sci. Rep.*, 2021, **11**, 1–13.

43 Z. Huang, Y. C. Chiew, W. D. Lu and S. Kawi, *Fluid Phase Equilib.*, 2005, **237**, 9–15.

44 A. Rojas, D. Cerro, A. Torres, M. J. Galotto, A. Guarda and J. Romero, *J. Supercrit. Fluids*, 2015, **104**, 76–84.

45 S. H. Khudaida, W. Y. Hsieh, Y. Z. Huang, W. Y. Wu, M. J. Lee and C. S. Su, *J. Supercrit. Fluids*, 2023, **194**, 105851.

46 C. Wang, T. Yan, T. Yan and Z. Wang, *J. Mol. Struct.*, 2023, **1279**, 134947.

47 L. López-Hortas, P. Rodríguez, B. Díaz-Reinoso, M. C. Gaspar, H. C. de Sousa, M. E. M. Braga and H. Domínguez, *J. Supercrit. Fluids*, 2022, **188**, 105652.

48 T. F. Gondo, M. Jönsson, E. N. Karlsson, M. Sandahl and C. Turner, *J. Chromatogr. A*, 2023, **1706**, 464267.

49 T. Do Dat, N. D. Hai, N. T. H. Nam, N. M. Thanh, N. T. T. Huyen, L. T. T. Duong, H. M. Nam and N. H. Hieu, *Biocatal. Agric. Biotechnol.*, 2023, **52**, 102824.

50 J. Mendez-Santiago and A. S. Teja, *Ind. Eng. Chem. Res.*, 2000, **39**, 4767–4771.

51 G. Sodeifian and S. A. Sajadian, *J. Supercrit. Fluids*, 2019, **149**, 79–87.

52 J. C. González, M. R. Vieytes, A. M. Botana, J. M. Vieites and L. M. Botana, *J. Chromatogr. A*, 2001, **910**, 119–125.

53 S. Soltani and S. H. Mazloumi, *Chem. Eng. Res. Des.*, 2017, **125**, 79–87.

54 C. Garlapati and G. Madras, *Thermochim. Acta*, 2010, **500**, 123–127.

55 A. Jouyban, M. Khoubnasabjafari and H.-K. Chan, *Chem. Pharm. Bull.*, 2005, **53**, 290–295.

56 S. A. Sajadian, M. Amani, N. Saadati Ardestani and S. Shirazian, *Arabian J. Chem.*, 2022, **15**, 103821.

57 M. Amani, N. S. Ardestani, A. Jouyban and S. A. Sajadian, *J. Supercrit. Fluids*, 2022, **190**, 105752.

58 A. Jouyban, H. K. Chan and N. R. Foster, *J. Supercrit. Fluids*, 2002, **24**, 19–35.

59 N. Esfandiari and S. A. Sajadian, *Fluid Phase Equilib.*, 2022, **556**, 113408.

60 M. Amani, N. Saadati Ardestani and N. Y. Majd, *J. CO$_2$ Util.*, 2021, **46**, 101465.

61 Y. Iwai, T. Fukuda, Y. Koga and Y. Arai, *J. Chem. Eng. Data*, 1991, **36**, 430–432.

62 G. Sodeifian, F. Razmimanesh and S. A. Sajadian, *J. Supercrit. Fluids*, 2019, **146**, 89–99.

63 M. Ota, Y. Hashimoto, M. Sato, Y. Sato, R. L. Smith and H. Inomata, *Fluid Phase Equilib.*, 2016, **425**, 65–71.

64 J. L. Li, J. S. Jin, Z. T. Zhang and X. M. Pei, *J. Supercrit. Fluids*, 2010, **52**, 11–17.

65 F. Chang, J. Jin, N. Zhang, G. Wang and H. J. Yang, *Fluid Phase Equilib.*, 2012, **317**, 36–42.

66 M. M. Azim, I. Ushiki, A. Miyajima and S. Takishima, *J. Supercrit. Fluids*, 2022, **186**, 105626.

67 N. S. Ardestani, M. Amani, M. Grishina and S. Shirazian, *Arabian J. Chem.*, 2022, **15**, 104371.

68 N. R. Foster, G. S. Gurdial, J. S. L. Yun, K. K. Liong, K. D. Tilly, S. S. T. Ting, H. Singh and J. H. Lee, *Ind. Eng. Chem. Res.*, 1991, **30**, 1955–1964.

69 S. H. Khudaida, Y. M. Chen, Y. F. Zheng, C. M. Hsieh and C. S. Su, *J. Supercrit. Fluids*, 2023, **192**, 105785.

70 O. Faraz, M. Poustchi, E. Nazari Denyani, P. Movahedi, F. Rajabi Kouchi and R. Shahriari, *J. Mol. Liq.*, 2022, **353**, 118809.

71 H. Bagheri, B. Notej, S. Shahsavari and H. Hashemipour, *Eur. J. Pharm. Sci.*, 2022, **177**, 106273.

72 S. Zabihi, S. Jamshidian, F. Borousan, A. Zeinolabedini Hezave, M. Pishnamazi, A. Marjani and S. Shirazian, *J. Chem. Thermodyn.*, 2021, **152**, 106271.